ELSEVIER

Bioelectrochemistry 51 (2000) 13–20

Bioelectrochemistry

www.elsevier.com/locate/bioelechem

Non-linear dielectric spectroscopy: antifouling and stabilisation of electrodes by a polymer coating

Andrew M. Woodward [a,*], E.A. Davies [b], S. Denyer [b], C. Olliff [b], Douglas B. Kell [a]

[a] *Institute of Biological Sciences, University of Wales, Cledwyn Building, Penglais, Aberystwyth, Dyfed, Wales SY23 3DD, UK*
[b] *Department of Pharmacy, University of Brighton, Brighton, Sussex BN2 4GJ, UK*

Received 17 May 1999; accepted 18 January 2000

Abstract

Non-linear dielectric spectroscopy (NLDS) has previously been shown to produce quantitative information that is indicative of the metabolic state of various organisms, by modeling the non-linear effects of their membranous enzymes on an applied oscillating electromagnetic field using supervised multivariate analysis methods. However, the instability of the characteristics of the measuring apparatus rendered the process temperamental at best in the laboratory and impractical for field use.

The main practical problem, of the non-stationarity of the electrode–solution interface and the ease with which the electrode surfaces are subject to protein fouling. It is addressed by applying a thin, electrically transparent antifouling coat to the electrodes. This reduces the interminable cleaning procedures previously required to prepare the electrodes for use, increases their usable lifetime before recleaning, and also improves the precision and linearity of multivariate models on NLDS data.

Keywords: Dielectric spectroscopy; Non-linear; Protein adhesion; Fermentation; Biotechnology; Polymer coating

1. Introduction

1.1. Non-linear dielectric spectroscopy (NLDS)

When a suspension of cells is exposed to a static electric field, or to an alternating electric field whose frequency is low relative to that of the classical β-dielectric dispersion, it does not penetrate to the interior of the cell, and is dropped almost entirely across the outer membrane of the cell, which is predominantly capacitive at these frequencies, and due to its thinness, causes a substantial amplification of the field across the membrane. (e.g., Refs. [1–3]). In consequence, anything internal to the cell is essentially electrically invisible to a low frequency electric field, but anything dielectrically active in the membrane may be expected to display properties associated with fields far stronger than that applied externally.

The dielectric response of biological tissue has long been assumed linear when the macroscopic exciting field is low, say < 0.1 V/cm as used typically; however, substantial non-linear phenomena in the form of harmonics of the fundamental are in fact produced for reasons discussed in Refs. [4,5], leading to the use of spectroscopy on the dielectric properties of the membranous enzymes actually to indicate and/or influence the metabolic state of cell suspensions [5–9].

Inhibitor and other studies indicated that, in yeast, the non-linear dielectric signal is due mainly to the H^+-ATPase located in the cells' plasma membrane [5,7], and, hence, NLDS may be used to quantify the use of glucose by yeast cells [9].

1.2. Electrode polarisation and fouling

In biological NLDS work, electrode polarisation is a serious problem at low frequencies (up to a few tens of hertz) where the biology typically reacts most strongly to

Abbreviations: Artificial neural network (NN); Genetic program(ming) (GP); Non-linear dielectric spectroscopy (NLDS); Partial least squares (PLS); Root mean squared error of prediction (RMSEP); Coefficient of variation (*C*)

* Corresponding author. Tel.: +44-1970-622111 ext. 1830; fax: +44-1970-622354.

E-mail addresses: azw@aber.ac.uk (A.M. Woodward), e.a.davies@bton.ac.uk (E.A. Davies), s.denyer@brighton.ac.uk (S. Denyer), c.j.olliff@bton.ac.uk (C. Olliff), dbk@aber.ac.uk (D.B. Kell).

0302-4598/00/$ - see front matter
PII: S0302-4598(00)00063-5

the electric field; and its fluctuations can be similar in size to, or bigger than, the small changes due to biological activity (e.g., upon glucose metabolism) [9]. It is, therefore, vital to control electrode polarisation as much as possible. Since harmonics fluctuate proportionally more than the fundamental, non-linear measurements, which concentrate on these harmonics, are much more sensitive to polarisation phenomena than are linear measurements, which concentrate exclusively on the relatively stable fundamental.

To obtain non-linear electrochemical reproducibility, we have found that electrode surfaces must be scrupulously clean, and this is very difficult to achieve. If any contamination is present, the biologically relevant signal may be unstable, distorted or concealed completely. Any results obtained will also be very dependent on the signal history! Only when electrodes are spotless will reasonably low-noise, repeatable results be obtained, although fluctuations will still occur. We find that these fluctuations occur on all timescales from slow drift over days, altering the effective characteristics of the sensing system between experiments, to second-to-second variations in polarisation harmonics, which affect the stability of the sensing system during a single reading.

Surfaces are very liable to contamination by many substances (proteins, sugars, lipids, etc.), which can bind to the electrode surface and distort results [10,11], proteins being particularly likely to cause trouble. The adhering material may insulate that part of the electrode surface covered; and whether insulative or not, it will significantly affect the form of the electrode polarisation impedance, and, consequently, this may alter the characteristics of the non-linear dielectric spectrometer during an experiment, or even a single spectrogram! So, the electrodes must be very carefully checked for surface interactions with any new chemical introduced into the test chamber before results obtained can be trusted.

Electrode cleaning to ensure repeatable non-linear dielectric spectra is a complex and empirical task, due to the lack of knowledge of the exact form of the causative mechanisms operating in the electrode/electrolyte interface. No repeatable and certain ways of obtaining a quiet and repeatable reference signal from an individual electrode surface have been found, but simple abrasion works best, in conjunction with applying a slowly alternating voltage to oxidise the surface contaminants and subsequently remove the oxidation products by the reduction half-cycle [12–14]. The electrode cleaning process is deemed successful when a repeatable, artefact-free signature can be obtained from a well-known and reliable reference system. In our case, a resting yeast suspension is used to provide reference signatures since its reliability and stability has been proven over time. When a clean, recognisable, repeatable, artefact-free harmonic signature can be obtained from a frequency sweep covering its frequency range, the electrodes are ready for use.

The maximum amplitude of the signal, which may be applied to the electrodes, is also limited since visible electrolysis occurs whenever the voltage much exceeds ± 1.5 V zero-to-peak; and at these voltages, the electrode surfaces are much more susceptible to contamination, and results become unstable.

Once clean, electrodes may stay stable for days, or become unstable within a few minutes. Continual control readings, performed as indicated above, are vital during any series of experiments to be sure that the electrode surface behaviour has not been substantially altered during the experiments, in which case, the results must be abandoned and the experiments repeated. This Byzantine process can make the process of obtaining a lengthy series of results with continually clean electrodes a nightmare.

1.3. Electrode coating

To prevent a protein from adhering to a metal surface, the surface can be coated with a sheet of polyethylene oxide (PEO) chains. This prevents the protein binding by steric repulsion, overpowering the attraction between the protein and the coating layer. Unfortunately, hydrophilic PEO does not adsorb effectively to metal surfaces. An alternative approach is to use poloxamers. These are a triblock copolymer consisting of PEO–polypropylene oxide (PPO)–PEO, in which two PEO chains are attached to a hydrophobic PPO structure. It is suspected that the hydrophobic PPO section attaches to the metal surface, which anchors the PEO chains [15]. Hence, a sheet of PEO–PPO–PEO molecules form on the electrode surface, with the PEO chains protruding into the solution. As the proteins approach this layer, they deform it, and the increase in energy required to create this deformation over the equilibrium energy of the sheet gives rise to steric repulsion and prevents further approach of the protein [16].

The length and surface density of the PEO chains affect both repulsion and adhesion [16]. Small protein molecules require a high surface density with the ends of the chains close together, whereas, larger proteins require a sparser covering (retaining the criterion that the spacing of the ends of the chains must always be much less than the protein size). The best repulsion is gained by the longest chain, which allows the optimum surface density [17].

2. Electrode stability

A Mexican Hat four-terminal gold electrode [5] was cleaned by abrasion in the old time-consuming way in Ref. [9]. The chamber was filled with 100 mM KCl and 60 spectrograms taken as described in Ref. [9] to study the stability of the electrode before coating.

The following control file was used:

```
5 9
0.5 0.75 1.0 1.25 1.5
10 17 31 56 100 177 316 562 1000
```

The top line of this signifies that all combinations of five voltages and nine sinusoidal frequencies will be generated in the sweep. The next line gives the chosen voltages in volts, and the final line gives the chosen frequencies in hertz.

At each voltage/frequency combination, a power spectrum, as in Fig. 1, was produced and the amplitudes of harmonics 1–5 of this spectrum were recorded to a disc. This leads to each sample (object) being composed of 225 *x*-variables and one reference *y*-variable.

Spectrograms were taken at the following time intervals in minutes:

Spectrograms 1–20 in 1-min intervals (1–20 min).
Spectrograms 21–40 in 2-min intervals (22–60 min).
Spectrograms 41–46 in 5-min intervals (65–90 min).
Spectrograms 47–49 in 10-min intervals (100–120 min).
Spectrograms 50–55 in 15-min intervals (135–210 min).
Spectrograms 56–60 in 30-min intervals (240–360 min).

The electrode was then coated with a PEO–PPO–PEO self-assembling monolayer by filing the electrode chamber with 2% w/v Synperonic PE/L64 [Fluka, http://www.fluka.com/] +2% w/v Lutrol P127 [BASF, http://www.basf.com/] and leaving to evaporate to dryness. The above time study was repeated and the results were compared.

The harmonics are separated and the coefficient of variation (C), is calculated for each voltage/frequency combination. The resulting third harmonic surface of C vs. frequency (f) vs. voltage (V) is given in Fig. 2a for the uncoated electrode, and in Fig. 2b for the coated electrode.

There is a slight but significant improvement in stability, but the most interesting feature is the similarity in the shape of the two plots. This similarity suggests that the coating is electrically transparent, and does not have a major effect on the electrical interface conditions between electrode and solution. This similarity is preserved through all harmonics 1–5.

If the mean level of these plots is taken to give a single figure as an index of stability, along with the equivalent for all the other harmonics for both the coated and uncoated electrode, then the mean of C can be compared in

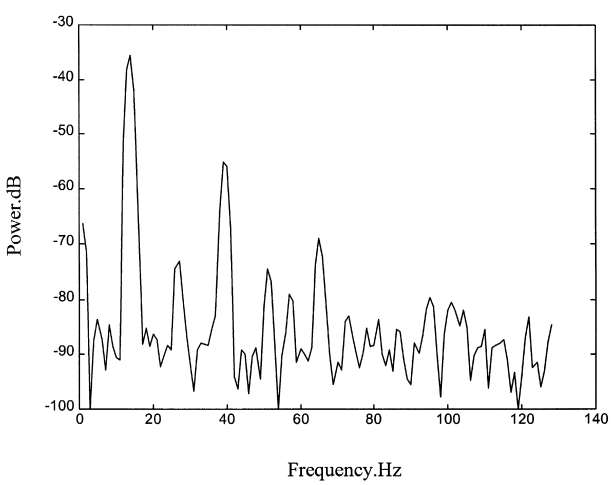

Fig. 1. Typical power spectrum produced by NLDS spectrometer. Here, the fundamental frequency is 13 Hz.

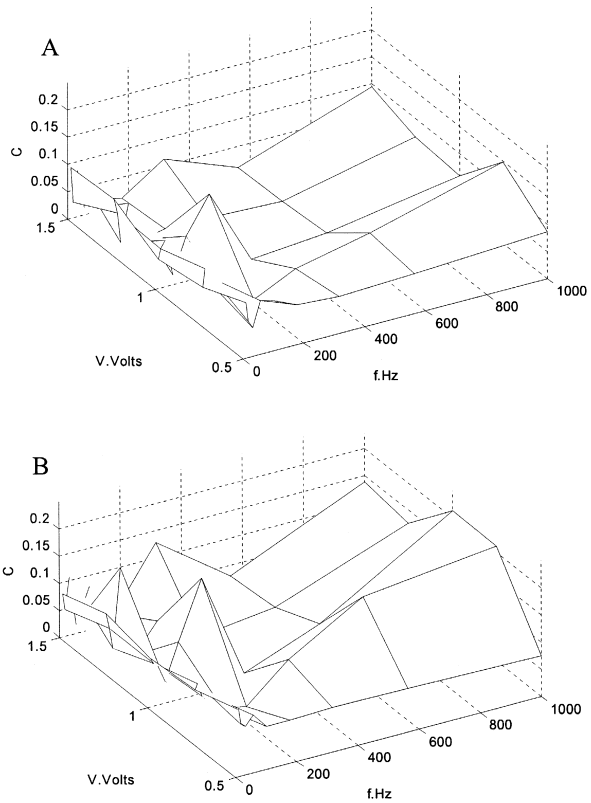

Fig. 2. Coefficient of variation of third harmonic of electrode response as a function of voltage and frequency for (A) uncoated gold electrode and (B) coated electrode.

Table 1
Overall mean value of C for each harmonic in coated and uncoated electrodes

Harmonic	Mean(C)	
A	Uncoated electrode 1	Coated electrode 1
1	0.008	0.007
2	0.09	0.07
3	0.09	0.06
4	0.10	0.08
5	0.08	0.07
B	Uncoated electrode 2	Coated electrode 2
1	0.02	0.006
2	0.10	0.08
3	0.12	0.08
4	0.10	0.08
5	0.09	0.06

Table 1A. Similar figures for a repeat experiment on a second electrode are given in Table 1B. This table demonstrates the improvement in stability due to the coating more clearly.

The similarity in form of the $C/V/f$ plots was also found to be repeated for all harmonics of the second electrode.

3. Detection of cell suspensions

Although the above figures suggest that the coating is electrically transparent, it is necessary to check that the coated electrode can still detect the world around it.

The standard suspension of *Saccharomyces cerevisiae* was prepared as follows. Freeze-dried yeast (Allinson's baking yeast, obtained locally) was rehydrated to 50 mg dry wt/ml in a solution of 1% yeast extract w/v in distilled water. This was allowed to stabilise overnight to allow the yeast to exhaust its endogenous energy stores, and enter a resting state before experiments were carried out. No cell growth occurred under the conditions used.

Yeast suspension was placed in the electrode chamber and a spectrogram was taken as above, but using the following control file:

```
3 10
1.0 1.25 1.5
5 10 15 20 25 30 35 40 45 50
```

With the first five harmonics at each voltage/frequency combination being recorded, this leads to each sample (object) being composed of 150 *x*-variables.

Then, a spectrogram of the supernatant was obtained with the conductivity exactly matched to that of the suspension with distilled water to compensate for the (insulative) volume fraction of the cells removed.

The process was repeated 30 times to produce 30 pairs of suspension and supernatant samples.

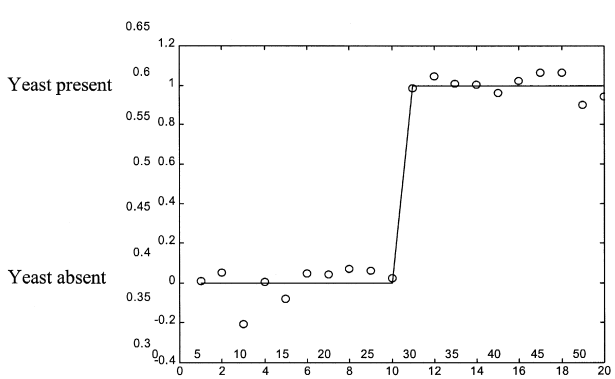

Fig. 3. Identification of the presence of cells in a suspension by coated electrode.

The 60 samples are split into three datasets. A partial least squares (PLS) [18] model was trained on one subset (the training set), and the validity of this model checked by predicting another (the validation set). The third unseen subset was then predicted. The unseen data set (the test set) was classified as yeast-present vs. yeast-absent, with 100% success, as shown in Fig. 3.

4. Quantification of glucose in a batch fermentation

Having checked that the electrode coating has not compromised the ability of the spectrometer to detect cell suspensions, the main purpose of this work is to study its ability to assist the spectrometer in modeling quantitative, metabolically significant parameters. The chosen parameter is glucose concentration in batch fermentation of baker's yeast.

Three batch fermentations were carried out on consecutive days with a coated electrode, exactly as in Ref. [9], using the same experimental protocols and data logging programs, to log non-linear dielectric spectrograms vs. time. Reference glucose concentration readings were provided by a Reflolux hand-held glucometer designed for at-home testing by diabetics. A repeat triplicate of fermentations was then carried out on another coated electrode.

The control file used was the same as for the detection of suspensions above, but differential spectrograms were also recorded. A spectrogram is taken using suspension in the electrode chamber, then an identical one taken using supernatant to give the spectrogram due to the electrode interface; and the latter of these was subtracted from the former to produce a spectrogram of cellular signal deconvolved from the electrode response. The suspension, supernatant, and difference spectra were recorded to separate files. This leads to each sample (object) being composed of 150 *x*-variables in each of the three files.

Five spectrograms were recorded with no glucose present, then glucose was added to a concentration of 170 mM, and spectrograms were taken every 2 min until the glucose was used up. For this yeast strain, this typically took 3 h from the addition of the glucose (Cell counting procedures showed that cell growth did not occur in these experiments.). Five subsequent spectrograms were recorded after the glucose levels in the suspension have reached zero.

The reference glucose levels were measured every third spectrogram with the Reflolux. We have measured the precision of this to be $\pm 10\%$. It has a detection range of 0.5 to 27 mM, so the higher-glucose-concentration samples used in yeast work are diluted before readings can be taken using this device.

Each batch fermentation produces a dataset. Median averaging in each variable with respect to sample number was used on these datasets as a robust weighing method to

remove the many large glitches in the datasets [9]. It relies on the fact that glucose-related phenomena change slowly during a fermentation, and any sudden changes are spuria. Consequently, using median averaged leading zeros smears the discontinuity at sample 6 (the addition of glucose), and hampers its modeling. Exploiting this argument, it was found in Ref. [9] that substituting the non-median-averaged leading zeros into the median averaged data gives the advantage of both well predicted (if noisier) leading zeros and a closely fitted glucose curve.

If PLS modeling is carried out for the three sets of data collected from one electrode using one dataset for the training set, a second dataset as the validation set and the last dataset as the test set, then six different combinations of prediction can be derived from the three datasets. This procedure was repeated on the datasets from the second electrode to produce six more predictions. The commonly used metric, the root mean square error of prediction (RMSEP) is used in forming and evaluating these PLS models [18].

Previous work has produced a typical prediction from three datasets of deconvolved difference spectra produced exactly as above but with uncoated electrodes [9], and is shown in Fig. 4. This prediction took many months of electrode cleaning and retaking of fermentation data until the electrode stayed stable, and with no significant fouling for the 3-day period necessary to produce these data! This forms the baseline, which the coating must improve upon.

As in all prediction figures in this paper, the measured reference data are shown as a solid line and the multivariate predictions are shown by individual points. The upper plot gives the relation of these points to the ideal 1:1 line of perfect prediction; and the lower plot shows the actual function being modeled along with the relation of the predicted points to this function.

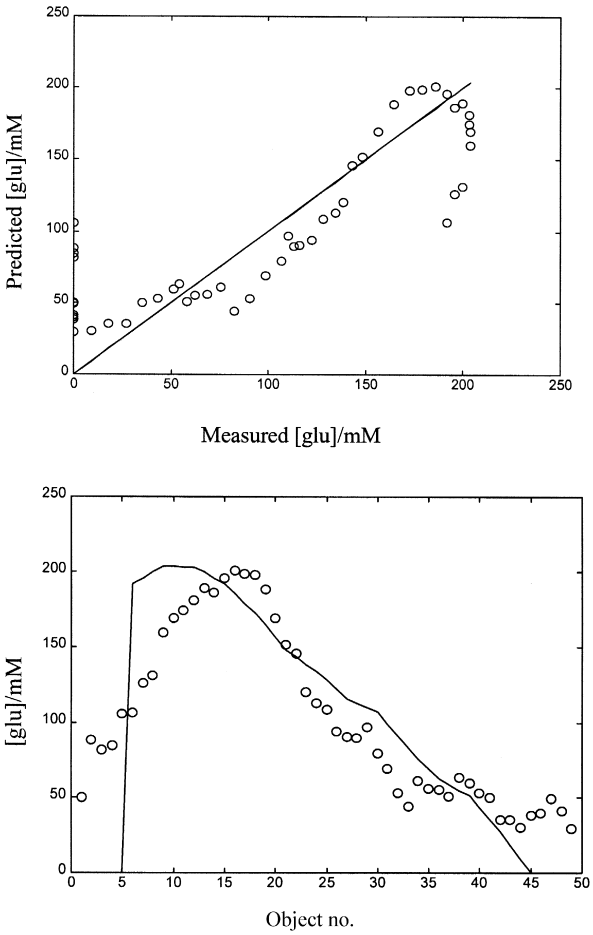

Fig. 4. PLS prediction between separate fermentations using uncoated electrodes and median averaged data (reproduced from Ref. [9]). The RMSEP is 41% at three factors.

The two representations are necessary since metabolically the yeast's resting state before the addition of glucose will not necessarily be identical to the resting state to which it returns after the glucose is used up, since storage polymers such as glycogen and trehalose will have been formed as a result of glucose metabolism [19–21]. On this basis, it may be expected that the leading zeros will be predicted less well if the model forms predominantly on the much larger section of finite- and post-glucose data. However, the prediction to some degree of the leading zeros is a vital check that the model is not merely forming on drifts and trends in the data, since data reflecting glucose utilisation are monotonic. If modeling were to occur merely on the basis of a trend, then, the leading zeros would be predicted to similar absolute levels as the initial glucose concentration, since the model would see them as contiguous with the high glucose readings. If merely modeling a trend in the data, the *x*-variables would be identical for samples taken both before and immediately after addition of glucose. Thus, the prediction of the leading zeros acts as a marker that the model is actually forming on a glucose-related response, and not merely on unconnected coincidental experimental drift [9].

There is also the likelihood that the trailing zeros will be overestimated since NLDS measures metabolism via the activity of the H^+-ATPase, and, hence, glucose levels indirectly; whereas, the Reflolux measures glucose directly. So, if there is significant metabolism of trehalose stored built-up from glucose during the fermentation, then, the reference method is telling the PLS model that there is no glucose; whereas, the NLDS is indicating continuous metabolism, so the PLS model can be expected to predict finite-glucose levels in this region. This means that any modeling method used has to model three different subsystems — the leading zeros, the finite glucose levels, and the trailing zeros — in order to produce a perfect prediction.

Returning to the new data from the coated electrodes, the worst of the 12 predictions was found to be similar to that of Fig. 4, while the best was excellent by any standard. The rest fell in a range in between, although they could usually be made excellent if a simple gain and/or dc term are added to the predictions. This is in accordance

with what would be expected if the impedance of the electrode interface drifted overnight.

It was also noticed that most of the predictions are more linear compared to those from the raw electrode, which were non-linear and required computationally expensive non-linear modeling techniques, such as neural networks (NN) or genetic programming (GP) for accurate modeling [9,22]. So, simple PLS on the data from the coated electrodes can give a good model and major improvements are not expected to be seen from NN or GP. This was indeed found to be the case, with GP giving almost identical but slightly cleaner versions of the predictions without improving precision significantly, and at the cost of days of computer time in comparison with seconds for a PLS model.

The worst PLS prediction is given in Fig. 5, while the best is shown in Fig. 6.

These predictions were obtained using suspension data directly with no deconvolution. Difference spectrograms produced slightly worse predictions, due to the doubling of the noise on the measurements inherent in the subtraction

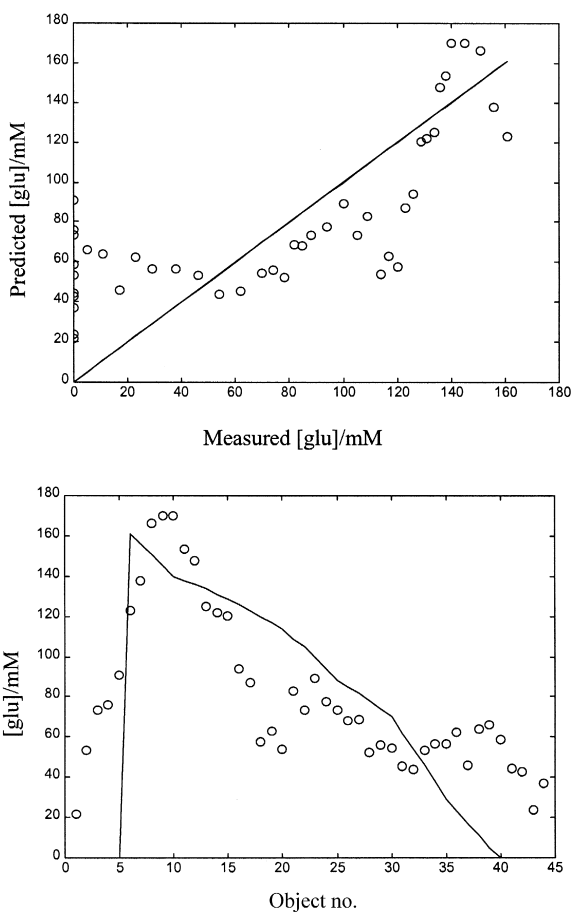

Fig. 5. Worst PLS prediction of the set of 12 produced by coated electrodes using median averaged data. The RMSEP is 53% at three factors.

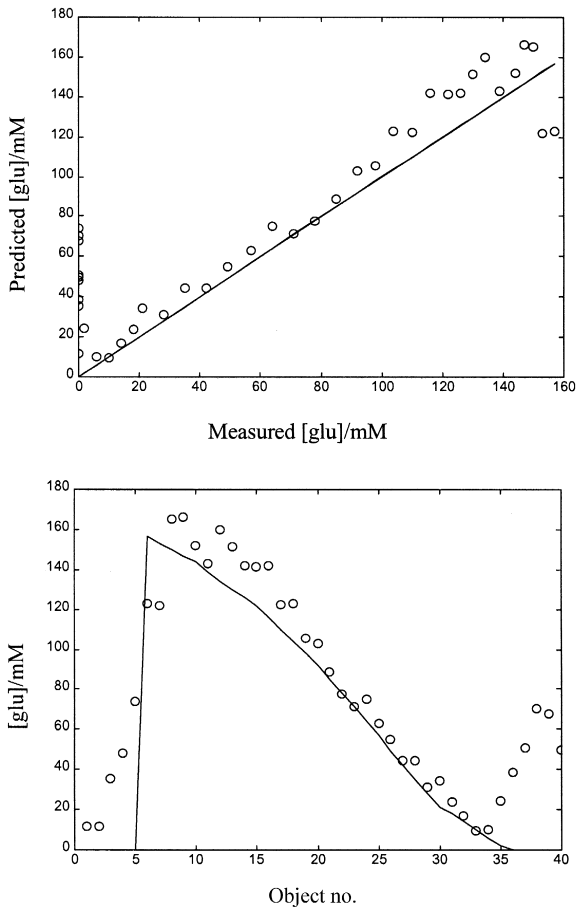

Fig. 6. Best PLS prediction of the set of 12 produced by coated electrodes using median averaged data. The RMSEP is 45% at six factors.

of suspension and supernatant spectrograms. The control predictions of supernatant data alone showed no modeling ability, confirming that reference supernatant readings are not required to produce valid predictions, and that the models are insensitive to simple conductivity effects. This allows future data collection to be greatly simplified (supernatants being difficult or impossible to obtain on-line in real-life applications) and speeded up, allowing a greater throughput of samples.

4.1. Long-term stability of coating

The long-term stability of the coating was tested over a period of 2 months, with further fermentations and predictions. After this period, one of the electrodes showed only minor deterioration, producing the prediction of Fig. 7 to compare with that of Fig. 6. The other electrode began to show slightly more significant deterioration, suggesting that this is close to the maximum period over which the coating can be considered stable enough for measurement.

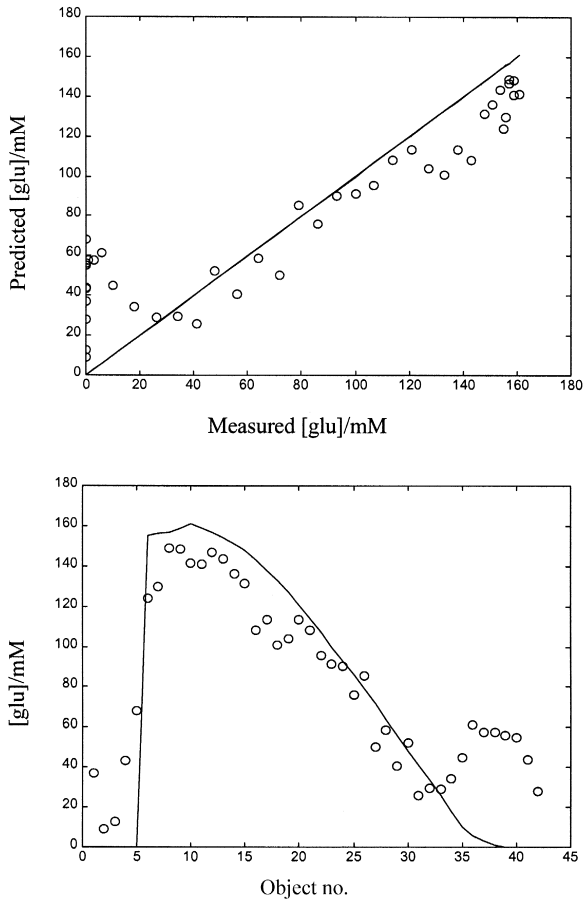

Fig. 7. PLS prediction of a fermentation taken 2 months after the application of the coating to the electrodes. The RMSEP is 38% at two factors.

It is recommended that, for reliable results, recoating be carried out at least monthly.

Note that the elevated predictions of the trailing zeros, suggesting trehalose metabolism as discussed above, hinder the RMSEP reflecting the precision of the rest of the prediction in the better cases. A comparison of Fig. 6 with Figs. 4 and 7 shows the shortcomings of single figure metric, such as the RMSEP for reflecting the fit of a curve, where a good fit with one portion modeled poorly can give a worse metric than one where every part is only modeled moderately. In these (and probably most multivariate modeling) cases, and in the absence of a convenient metric indicating the 'shape' of the prediction, there is no substitute for simply eyeballing the fit. Automatic optimum training algorithms based on detecting the RMSEP of the validation set can (and do) easily go astray in situations other than the modeling of Gaussian-distributed data for which the assumptions of the RMSEP are derived, since the minimum RMSEP on the validation set may not correspond to the 'best' fit according to criteria required by the problem at hand.

5. Conclusions

It must be stressed that the production of the PLS predictions of fermentation data shown in this paper contrast very strongly with those of Fig. 4 obtained in previous work for an uncoated electrode in that, as has been stated above, the uncoated electrode only produced these results after an unfeasibly long process of cleaning, testing and recleaning. The data from the coated electrode were produced simply by coating an electrode and using it. This constitutes a huge advance in taking NLDS from merely an interesting laboratory phenomenon towards a practical on-line measurement technique. Any improvement in precision of predictions is the icing on this cake.

A general (though not startling) increase in the precision of the predictions between datasets is produced as would be expected from a coating that behaves primarily as an antifouling layer while being electrically transparent, and which produces a limited improvement in stability of the polarisation layer at the electrode–solution interface. However, there is a considerable decrease in the nonlinearity of the models, thus, formed. This improvement in linearity allows simpler and much faster modeling methods to be used with a huge savings in computer load.

Also, the suggestion in Ref. [9] that good and valid predictions can be obtained without the requirement for supernatant spectra to be deconvolved is confirmed by the results presented here.

The ability to carry out NLDS measurements without the interminably empirical electrode cleaning process described above brings the technique of NLDS into the realms of practicality, at least as a laboratory tool.

Acknowledgements

AMW and DBK thank Wellcome Trust, under the terms of the Sir Henry Wellcome SHoWCASe Award scheme for financial support.

References

[1] R. Pethig, D.B. Kell, The passive electrical properties of biological systems: their significance in physiology, biophysics and biotechnology, Phys. Med. Biol. 32 (1987) 933–970.
[2] T.Y. Tsong, R.D. Astumian, Absorption and conversion of electric field related energy by membrane-bound ATPases, Bioelectrochem. Bioenerg. 15 (1986) 457–476.
[3] U. Zimmermann, Electric field mediated cell fusion and related electrical phenomena, Biochim. Biophys. Acta 694 (1982) 227–277.
[4] D.B. Kell, R.D. Astumian, H.V. Westerhoff, Mechanisms for the interactions between nonstationary electric fields and biological systems: I. Linear dielectric theory and its limitations, Ferroelectrics 86 (1988) 59–78.
[5] A.M. Woodward, D.B. Kell, On the nonlinear properties of biologi-

cal systems — *Saccharomyces cerevisae*, Bioelectrochem. Bioenerg. 24 (1990) 83–100.
[6] A.M. Woodward, D.B. Kell, On the relationship between the nonlinear dielectric-properties and respiratory activity of the obligately aerobic bacterium *Micrococcus luteus*, Bioelectrochem. Bioenerg. 26 (1991) 423–439.
[7] A.M. Woodward, D.B. Kell, Confirmation by using mutant strains that the membrane-bound H^+-Atpase is the major source of nonlinear dielectricity in *Saccharomyces cerevisiae*, FEMS Microbiol. Lett. 84 (1991) 91–95.
[8] A.M. Woodward, D.B. Kell, Dual-frequency excitation — a novel method for probing the nonlinear dielectric-properties of biological-systems, and its application to suspensions of *Saccharomyces cerevisiae*, Bioelectrochem. Bioenerg. 25 (1991) 395–413.
[9] A.M. Woodward, A. Jones, X.-Z. Xhang, J.J. Rowland, D.B. Kell, Rapid and non-invasive quantification of metabolic substrates in biological cell suspensions using non-linear dielectric spectroscopy with multivariate calibration and artificial neural networks, Bioelectrochem. Bioenerg. 40 (1996) 99–132.
[10] T.K. Chen, Y.Y. Lau, D.K.Y. Wong, A.G. Ewing, Pulse voltammetry in single cells using platinum microelectrodes, Anal. Chem. 64 (1992) 1264–1268.
[11] C.D. Ferris, Introduction to Bioelectrodes, Plenum, 1974.
[12] L.A. Larew, D.C. Johnson, Concentration dependence of the mechanism of glucose oxidation at gold electrodes in alkaline media, J. Electroanal. Chem. 262 (1989) 176–182.
[13] S. Hughes, D.C. Johnson, Triple-pulse amperometric detection of carbohydrates after chromatographic separation, Anal. Chim. Acta 149 (1983) 1–10.
[14] G.G. Neuburger, D.C. Johnson, Pulsed coulometric detection of carbohydrates at a constant detection potential at gold electrodes in alkaline media, Anal. Chim. Acta 192 (1987) 205–213.
[15] P. Claesson, Poly(ethylene oxide) surface coatings: relations between intermolecular forces, layer structure and protein repellency, Colloids Surf., A 77 (1993) 109–118.
[16] S.I. Jeon, J.H. Lee, J.D. Andrade, P.G. de Gennes, Protein-surface interactions in the presence of polyethylene oxide — 1. Simplified theory, J. Colloid Interface Sci. 142 (1991) 149–158.
[17] S.I. Jeon, J.D. Andrade, Protein–surface interactions in the presence of polyethylene oxide — 2. Effect of protein size, J. Colloid Interface Sci. 142 (1991) 159–166.
[18] H. Martens, T. Næs, Multivariate Calibration, Wiley, Chichester, 1989.
[19] S.H. Lillie, J.R. Pringle, Reserve carbohydrate metabolism in *Saccharomyces cerevisiae*: response to nutrient limitation, J. Bacteriol. 143 (1980) 1384–1394.
[20] J.C. Slaughter, T. Nomura, Intracellular glycogen and trehalose contents as predictors of yeast viability, Enzyme Microb. Technol. 14 (1992) 64–67.
[21] J.M. Thevelein, S. Hohmanm, Trehalose synthase: guard to the gate of glycolysis in yeast?, TIBS 20 (1995) 3–10.
[22] A.M. Woodward, R.J. Gilbert, D.B. Kell, Genetic programming as an analytical tool for non-linear dielectric spectroscopy, Bioelectrochem. Bioenerg. 48 (1999) 389–396.